

GENERAL ATOMIC
DIVISION OF **GENERAL DYNAMICS**

MASTER

GA-1787

MEASUREMENTS OF HEAT-TRANSFER COEFFICIENTS, FRICTION
FACTORS, AND VELOCITY PROFILES FOR AIR FLOWING
PARALLEL TO CLOSELY SPACED RODS

November 28, 1960

DISCLAIMER

This report was prepared as an account of work sponsored by an agency of the United States Government. Neither the United States Government nor any agency Thereof, nor any of their employees, makes any warranty, express or implied, or assumes any legal liability or responsibility for the accuracy, completeness, or usefulness of any information, apparatus, product, or process disclosed, or represents that its use would not infringe privately owned rights. Reference herein to any specific commercial product, process, or service by trade name, trademark, manufacturer, or otherwise does not necessarily constitute or imply its endorsement, recommendation, or favoring by the United States Government or any agency thereof. The views and opinions of authors expressed herein do not necessarily state or reflect those of the United States Government or any agency thereof.

DISCLAIMER

Portions of this document may be illegible in electronic image products. Images are produced from the best available original document.

GENERAL ATOMIC
DIVISION OF
GENERAL DYNAMICS

JOHN JAY HOPKINS LABORATORY FOR PURE AND APPLIED SCIENCE

P.O. BOX 608, SAN DIEGO 12, CALIFORNIA

GA-1787

**MEASUREMENTS OF HEAT-TRANSFER COEFFICIENTS, FRICTION
FACTORS, AND VELOCITY PROFILES FOR AIR FLOWING
PARALLEL TO CLOSELY SPACED RODS**

by

Luther D. Palmer and Leonard L. Swanson

Submitted for presentation at the Second International Heat Transfer Conference, to be held at Boulder, Colorado, August 28-September 1, 1961, and for publication in the Proceedings of the Conference.

Project 32.230
Contract AT(04-3)-314

November 28, 1960

ABSTRACT

The design of gas-cooled reactors with solid-rod fuel elements is predicated on knowledge of the pressure-drop and heat-transfer characteristics within the reactor core. There have been very few experimental investigations of systems in which the gas flows parallel to closely spaced rods. Therefore, heat-transfer and fluid-dynamic studies were made with air flowing parallel to the rods of a seven-rod cluster. The parallel rods were equally spaced in a triangular array with a 1.015 ratio of center-to-center distance to rod diameter, the rod surfaces forming flow passages of tricuspid-shaped cross section. Average and local heat-transfer film coefficients, pressure drops, and velocity profiles were measured under established hydrodynamic conditions.

The measured average heat-transfer film coefficients were approximately equal to those for smooth round ducts; however, the peripheral variation of the local coefficients at a Reynolds number of 20,000 was 0.5 to 1.3 of the average values. The data were obtained under the following forced-convection conditions:

Reynolds number 10,000 to 60,000

Rod heat flux 400 to 1,000 Btu/(hr)(ft²)

Rod surface temperature 100° to 160° F

Fanning friction factors calculated from static-pressure-drop measurements made along the length of a flow passage were approximately 5% higher than those for smooth round ducts over a Reynolds number range of 3,000 to 30,000.

The velocity structure in the flowing gas was determined at a Reynolds number of 20,000. The peripheral variation of the ratio of local to bulk mean velocity was found to be very nearly equal to the ratio of the local to average heat-transfer coefficient. This agreement of the local and average heat-transfer data is to be expected from the analogy between fluid friction and heat transfer.

MEASUREMENTS OF HEAT-TRANSFER COEFFICIENTS, FRICTION
FACTORS, AND VELOCITY PROFILES FOR AIR FLOWING
PARALLEL TO CLOSELY SPACED RODS^{*}

by

Luther D. Palmer[†] and Leonard L. Swanson[†]

INTRODUCTION

Recent designs of high-temperature heat exchangers and nuclear reactors incorporate coolant-flow lengthwise passages formed by the spaces between parallel rods or tubes in closely spaced equilateral arrays. The resulting coolant shear stress distribution is quite different from that found in ordinary ducts and may cause unusual heat-transfer rates within the flow passages, as well as pressure drops through the passages. Previous mathematical analyses^{(1)(2)**} predict large circumferential variations of the friction and average heat-transfer film coefficients from the accepted empirical correlations. However, certain experimental studies,⁽³⁻⁷⁾ in which the rods are widely spaced, indicate that the circumferential variation in the local heat-transfer film coefficients is much less than predicted. These experimental studies indicate, also, that conventional correlations may be used to calculate the friction and average heat-transfer film coefficients. A question then arises as to the heat-transfer rates within and pressure drops through the flow passages under conditions of closely spaced rods, that is, when the gaps between the rods are of the order of 0.01 of the rod diameter. Because of the difficulty of representing forced convection and hydrodynamic phenomena for turbulent flow in mathematical form, experimental measurements must be made. Two air-flow systems (see Fig. 1)

^{*} These studies were sponsored by the U. S. Atomic Energy Commission, under Contract No. AT(04-3)-314.

[†] John Jay Hopkins Laboratory for Pure and Applied Science, General Atomic Division of General Dynamics Corporation, P. O. Box 608, San Diego 12, California.

^{**} References are listed at the conclusion of this paper.

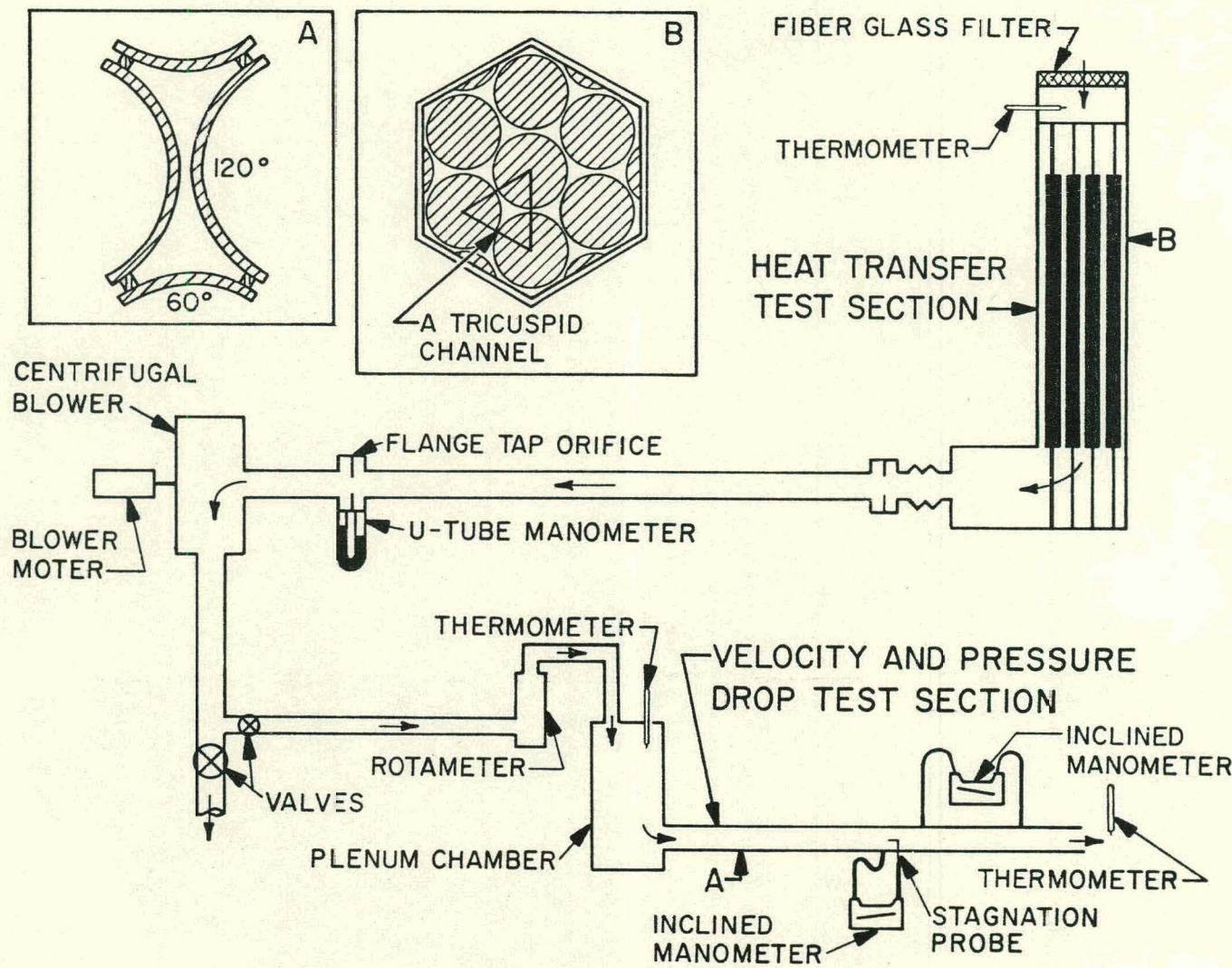


Fig. 1--Schematic drawing of the heat transfer and velocity and pressure drop test systems, showing cross-section views of each test section

were used to make these measurements, the pressure drops and velocities being measured under isothermal conditions in a dual tricuspid flow channel and the constant-wall-temperature heat-transfer coefficients being measured in a seven-rod cluster.

DESCRIPTION OF SYSTEMS*

Velocity and Pressure-drop Test System

For this system, air was delivered by a centrifugal blower through a rotameter and a plenum chamber to a dual-channel test passage from which the air was vented to the atmosphere. This test passage (see Insert A in Fig. 1) was formed by joining two 120° and two 60° circumferential segments of aluminum tubing. The leading edges of the tubing were rounded and were positioned within the plenum chamber so as to reduce entrance disturbances. The inside surfaces of the flow passage were machined and hand-finished to correspond to the surfaces of the rods in the heat-transfer lattice.

Static pressure taps were located at points 110 and 134 equivalent diameters downstream from the channel entrance. The stagnation probe penetrated the channel wall upstream from the static pressure taps. A thermometer in the plenum chamber was used to measure the temperature of the flowing air.

Heat-transfer Test System

The heat-transfer system utilized the same blower as the velocity and pressure-drop system, being connected to the inlet side of the blower. Air from the room (which served as an infinitely large plenum) was drawn through the heated test lattice, was passed through a calibrated orifice, and was then vented to the atmosphere by means of valve arrangements.

The test lattice consisted of seven rods spaced in an equilateral cluster within a hexagonal chamber, with circumferential segments of

* Further descriptive details of the experimental systems are presented in an Addendum to this paper.

tubing attached to the chamber walls to simulate the adjacent rods of a large array (see Insert B of Fig. 1). A thermometer for measuring the inlet-air mean temperature was located at the entrance of the chamber below a fiberglass filter, which served to remove particles from the air and to suppress flow disturbances caused by air currents within the room.

Each rod of the test lattice was composed of three contiguous hollow aluminum cylinders: (1) a thin-walled, upstream flow development portion; (2) a thick-walled, heated portion; and (3) a thin-walled, downstream exit portion. The heated portion of each rod contained a helical electrical resistance heater tightly wound on a stainless steel pipe which passed through this thick-walled aluminum cylinder. The asbestos-insulated, stainless-steel-sheathed heater wire was in firm contact with the inner surface of the cylinder, and calibrated copper-constantan thermocouples were embedded in the rod surface along this heater portion.

The central rod of the seven-rod cluster contained additional calibrated surface thermocouples, as well as a small temperature-controlled surface heater installed within the rod wall in such a manner that its surface was continuous with that of the rod itself. The electrical leads were exited through a hole located between the resistance heater and the surface of the rod in order to avoid subjecting the wire to a temperature gradient which would result in heat transfer along the wires.

EXPERIMENTAL TECHNIQUE*

Velocity and Pressure Drop

The static pressure losses in the dual-channel flow passage were measured at entrance lengths of 110 and 134 equivalent diameters over a Reynolds number range of from 3,000 to 30,000 for air at $\sim 90^{\circ}\text{F}$. The stagnation pressures were measured at an entrance length of 105 equivalent diameters for a Reynolds number of 20,000 as functions of the perpendicular

* Definitions of notation used are listed at the end of this paper.

distances from the channel wall at peripheral positions of 0° , 10° , 15° , 20° , and 30° . The Reynolds numbers for both the static-pressure and the stagnation-pressure measurements were based on the total flow and the equivalent diameter of the dual-channel passage.

Heat Transfer

The constant wall-temperature heat-transfer film coefficients, both local, as a function of peripheral position, and average, were measured and correlated as a function of a Reynolds number based on the total flow and equivalent diameter of the test lattice.

The average heat-transfer film coefficients were calculated by using the equation

$$\bar{h} = \frac{\bar{q}}{A(t_{s,x} - \frac{x}{X} \frac{\bar{q}}{mc_p} - t_{m,in})} \quad (1)$$

The rod surface temperatures, $t_{s,x}$, were measured at three hydrodynamic entrance lengths of 38.4, 57.3, and 74.0 equivalent diameters; the upstream heated length of each was 22.2 equivalent diameters. The total flow rate through the lattice, m , which necessitated the use of the total heating rate, was used because of the difficulty involved in measuring the individual flow rate through each passage. Velocity measurements with pitot-static probes located at the center of each of the tricuspid passages indicated less than 2% difference in flow rate. Comparison of these velocity measurements with the velocity profiles measured in the velocity and pressure-drop test passage, showed that the indicated flow rates were within 4% of those calculated using the total flow and cross-sectional area of the lattice.

The local circumferential variations of the heat flux were determined from measurements of the electrical power necessary for equalizing the temperature of the small heater surface to that of the adjacent tube wall while the central rod was rotated about its longitudinal axis, the small heater

passing from the smallest to the largest interstice between the rods. This technique is valid if (1) the rod containing the small heater has a circumferentially constant wall temperature and (2) the small heater is either thermally insulated or guard-heated and calibrated. The first condition was satisfied: An electrical analog plot indicated that in the worse case measured (where the simulated circumferential variation of the heat flux was 0.5 to 1.3 and the small heater was positioned at the largest gradient of the surface heat flux) the maximum circumferential temperature difference was 1.8°F and the temperature drop across the surface heater was 0.7°F . The second requirement was fulfilled by having a guard heater below the surface heater to prevent heat losses through the lead wires and by calibrating the central rod containing the small surface heater in an annulus system under proper temperature and heating conditions.* Integration of the local heat flux at entrance lengths of 38.4, 57.3, and 74.0 equivalent diameters yielded average values which were within $\pm 10\%$ of those determined from the overall lattice measurements. Errors in measurement which could be attributed to the technique were minimized, in dimensionless comparisons, by using the average heat flux obtained by integrating the peripheral values. Consequently, the ratio of local to average heat flux can be considered equivalent to the local-to-average film coefficients.

RESULTS OF MEASUREMENT

Velocity and Pressure Drop

The static pressures were correlated in dimensionless form (Fanning friction coefficient) as a function of channel Reynolds number (see Fig. 2). The values, which have a maximum possible range of error of 6%, are between those for smooth ducts and those for commercial pipe.⁽⁸⁾ Published correlations of pressure losses with air flowing through smooth tubes⁽⁹⁾ are also shown in Fig. 2 for comparison. It appears that the pressure losses

* See Addendum.

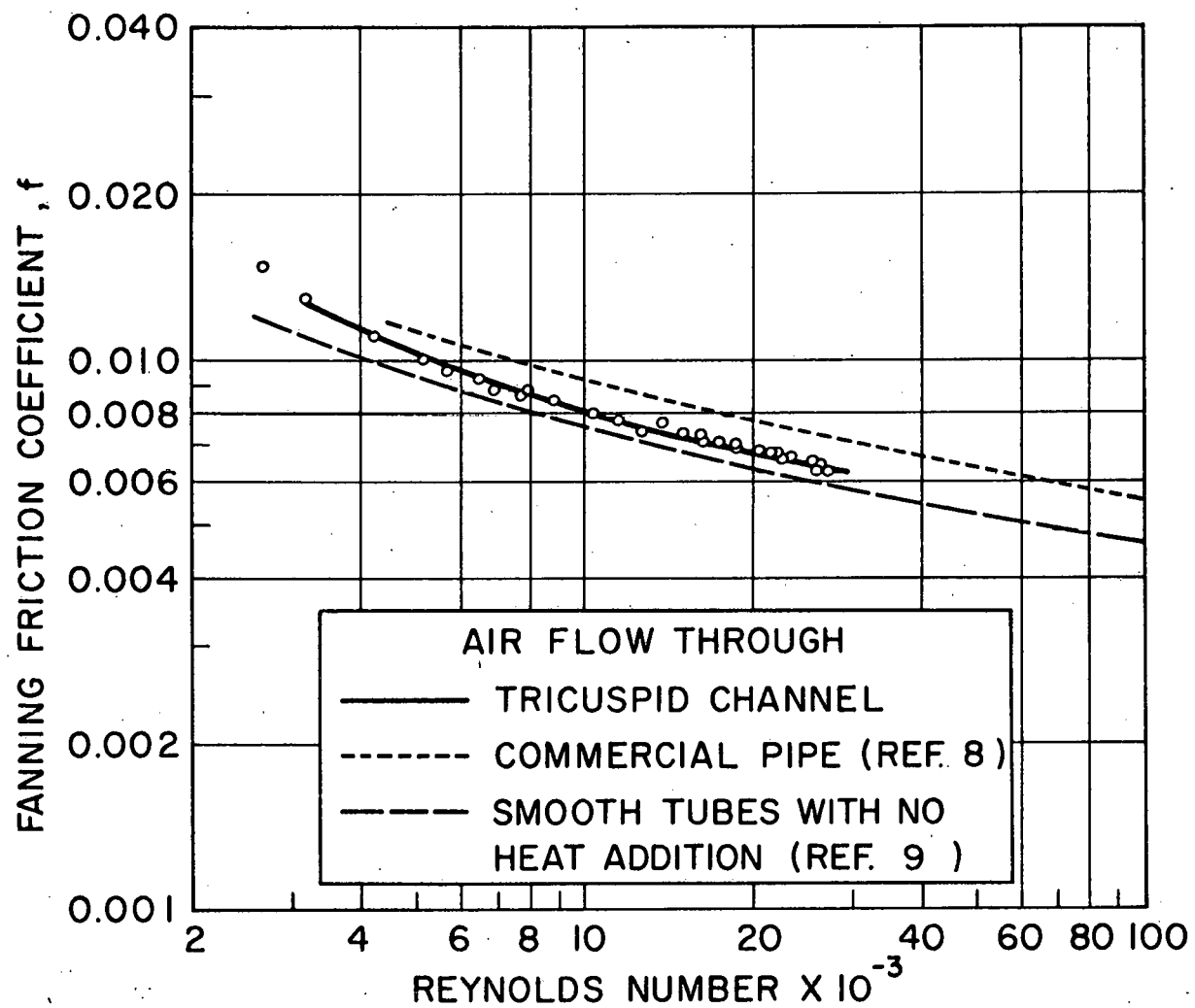


Fig. 2--Measured Fanning friction as a function of Reynolds number

reported here are consistent with other air-flow measurements.

The stagnation pressures for air flowing at a Reynolds number of 20,000 were converted to velocities, which are shown in Fig. 3 as a function of dimensionless distance from the duct wall with peripheral position as a parameter. An error analysis of these measurements indicates a maximum possible error of 3% in the pressure measurements and a possible 5% in the distance measurements.

Heat Transfer

The average heat-transfer data in dimensionless form are shown in Fig. 4 as a function of Reynolds number. The values tend to be below the Dittus-Boelter relation which applies to fluid forced convection in smooth pipes; however, upon comparison with others,^(9, 10) the data appear to be consistent with previous measurements.

The measured peripheral variations of the local heat-transfer film coefficients are shown in Fig. 5 as a function of peripheral position with the Reynolds number as a parameter. The values obtained by graphically integrating these curves were within $\pm 10\%$ of the averages calculated from the over-all measurements.

It is interesting to note the insensitivity of the data to guard heating, which indicates that the conduction heat losses from the surface heater, in the absence of guard heating, are nearly uniform with respect to peripheral position.

An important requirement of this study was that the measurements be made under stabilized hydrodynamic conditions; therefore, three sets of upstream flow development sections of different lengths were used to create varying entrance lengths. The three lengths of the flow development sections resulted in the small surface heater being located at 38.4, 57.3, and 74.0 equivalent diameters from the entrance. The measured heat-transfer rates shown in Fig. 4 demonstrate that at Reynolds numbers greater than 20,000 there is no appreciable difference in the values for

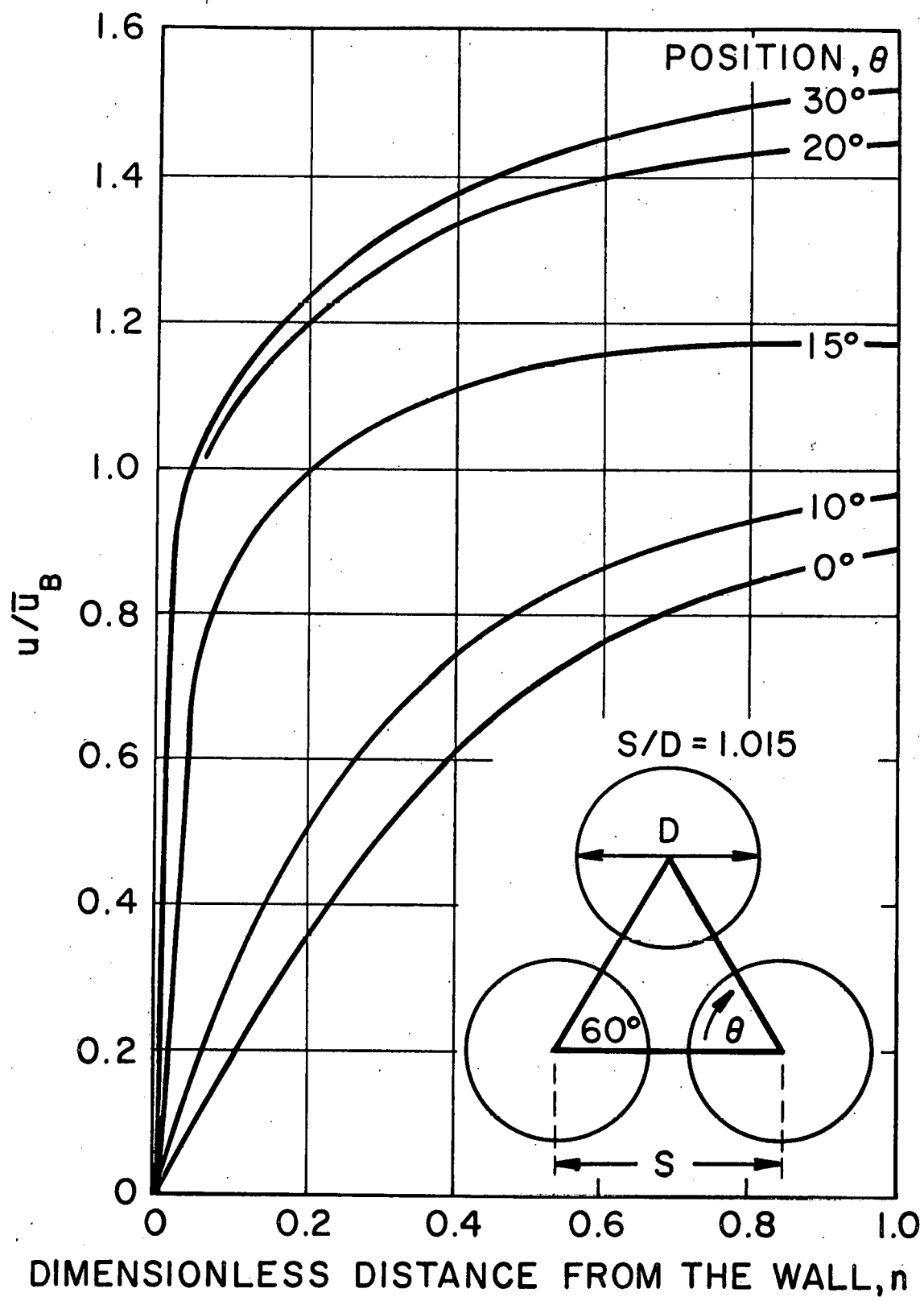


Fig. 3--Velocity profile at a Reynolds number of 20, 000

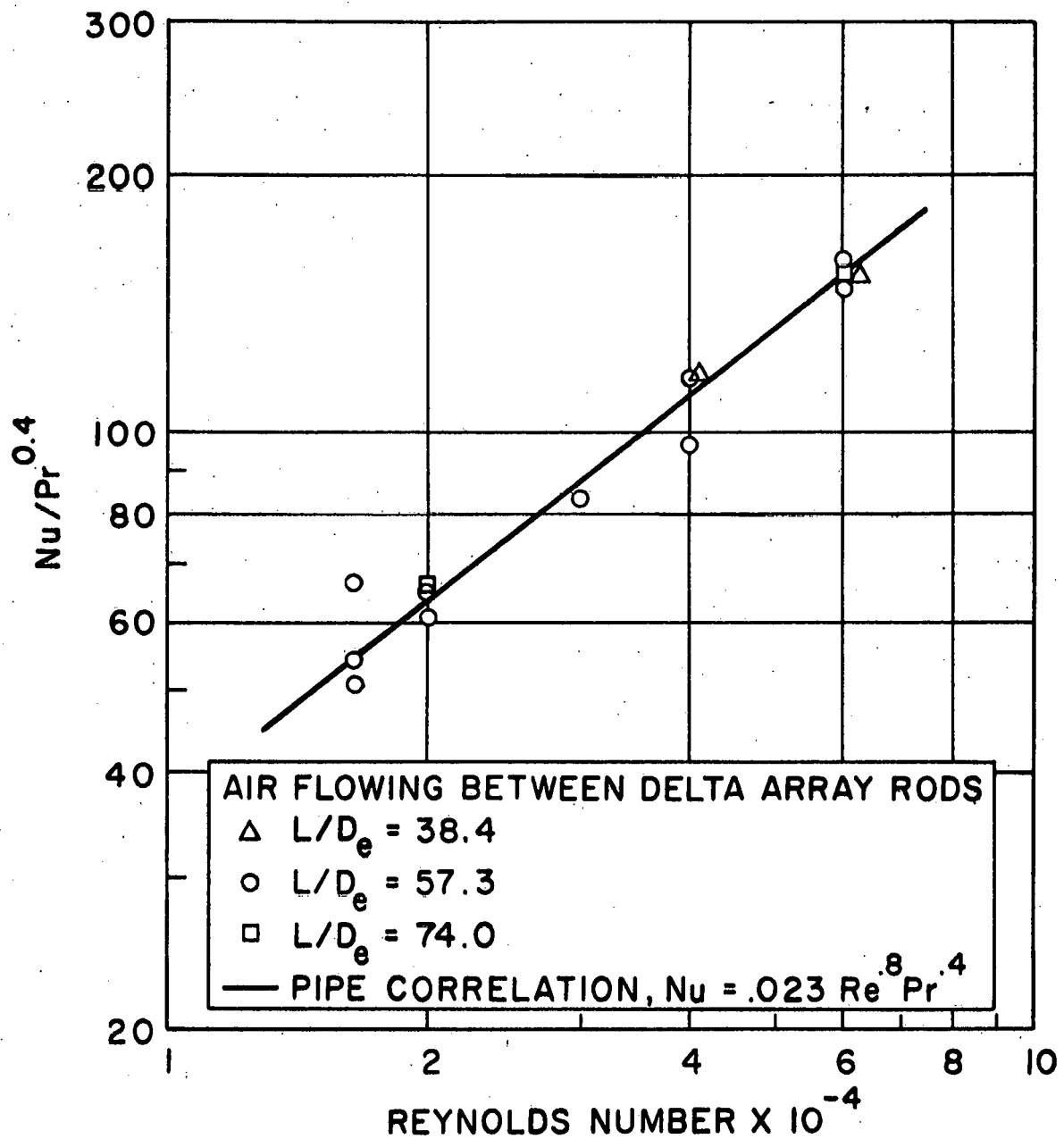


Fig. 4--Measured over-all heat-transfer rates from the rod surface to air, as a function of Reynolds number

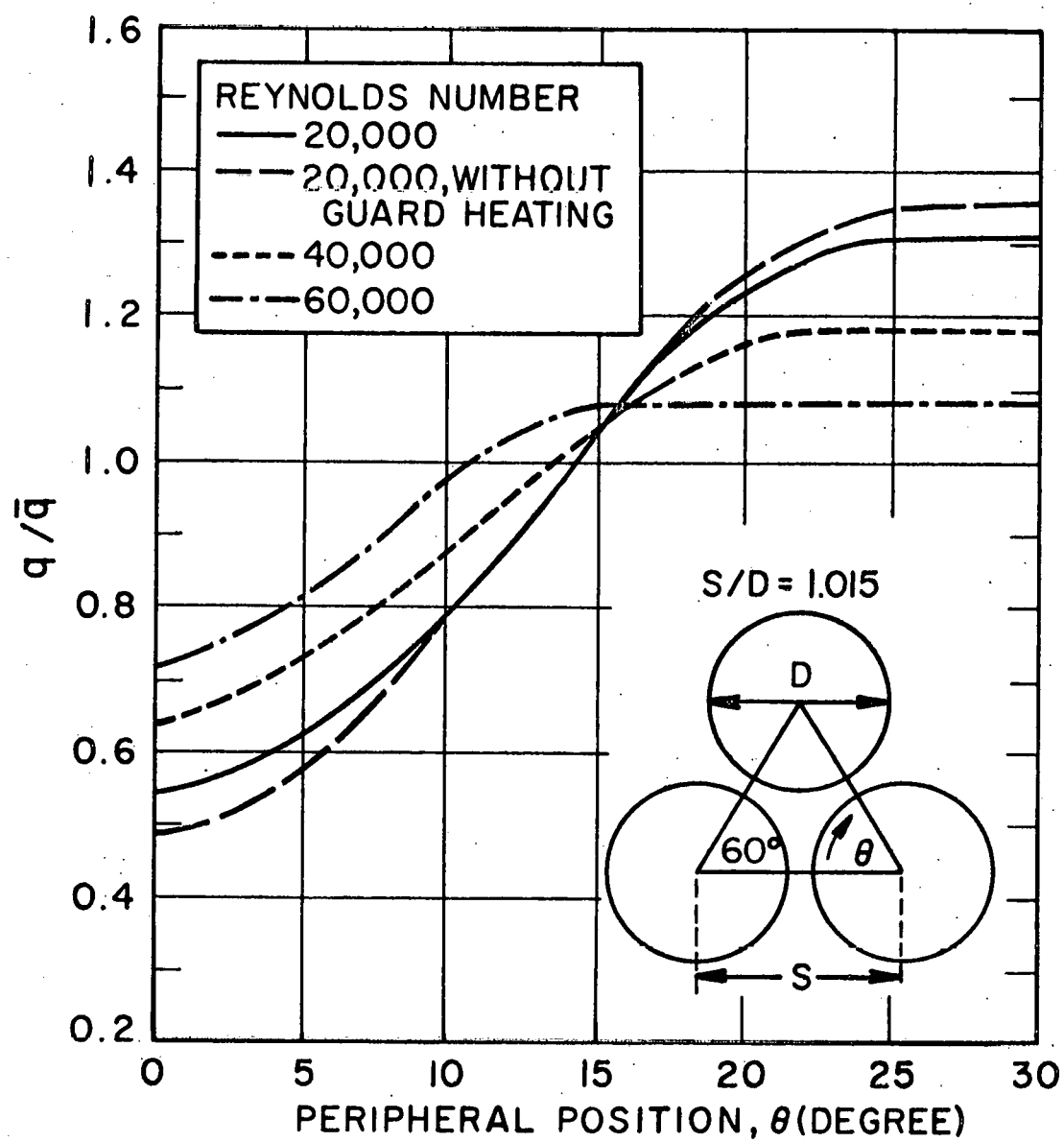


Fig. 5--Peripheral variation of the measured heat-transfer rates

the three entrance lengths. It appears that the correlation presented here can be used in heat-transfer calculations for cases far downstream where fully developed flow is known to exist.

DISCUSSION OF RESULTS

The results of this investigation lend credence to the practice of using the equivalent-diameter concept in conventional heat-transfer and fluid-friction correlations for the purpose of determining the over-all characteristics of flow along tube bundles with a ratio of pitch to rod-diameter of 1.015. However, no such empirical relations exist which describe the peripheral variation of the local heat-transfer coefficient under these conditions. This nonuniformity of heat conductance is, therefore, experimentally indicated as a serious problem in the use of this type of solid-to-gas heat-transfer process.

A comparison of the average heat-transfer and friction film coefficients can be made by utilizing the Colburn function, which is usually given as

$$f/2 = St Pr^{2/3} \quad (2)$$

However, previous experiments with gases have yielded values of $f/2$ which are $\sim 10\%$ higher than the $St Pr^{2/3}$ term. This difference is also found in the measurements presented here, as shown in Fig. 6, and is in agreement with an analysis published in Ref. 11.

A comparison of the ratio of the local mean velocity to the duct mean velocity and the ratio of the local to mean heat-transfer coefficients is shown in Fig. 7 as a function of peripheral position. The local mean velocities ($\bar{u}_{r,\theta}$) were obtained by integrating the velocity profiles normal to the rod surface with respect to the distance from the wall to the line of symmetry within the duct. The dependence of the local heat-transfer rates on the local mean velocities is quite evident.

The data presented here for air flowing under the described conditions can be summarized as follows:

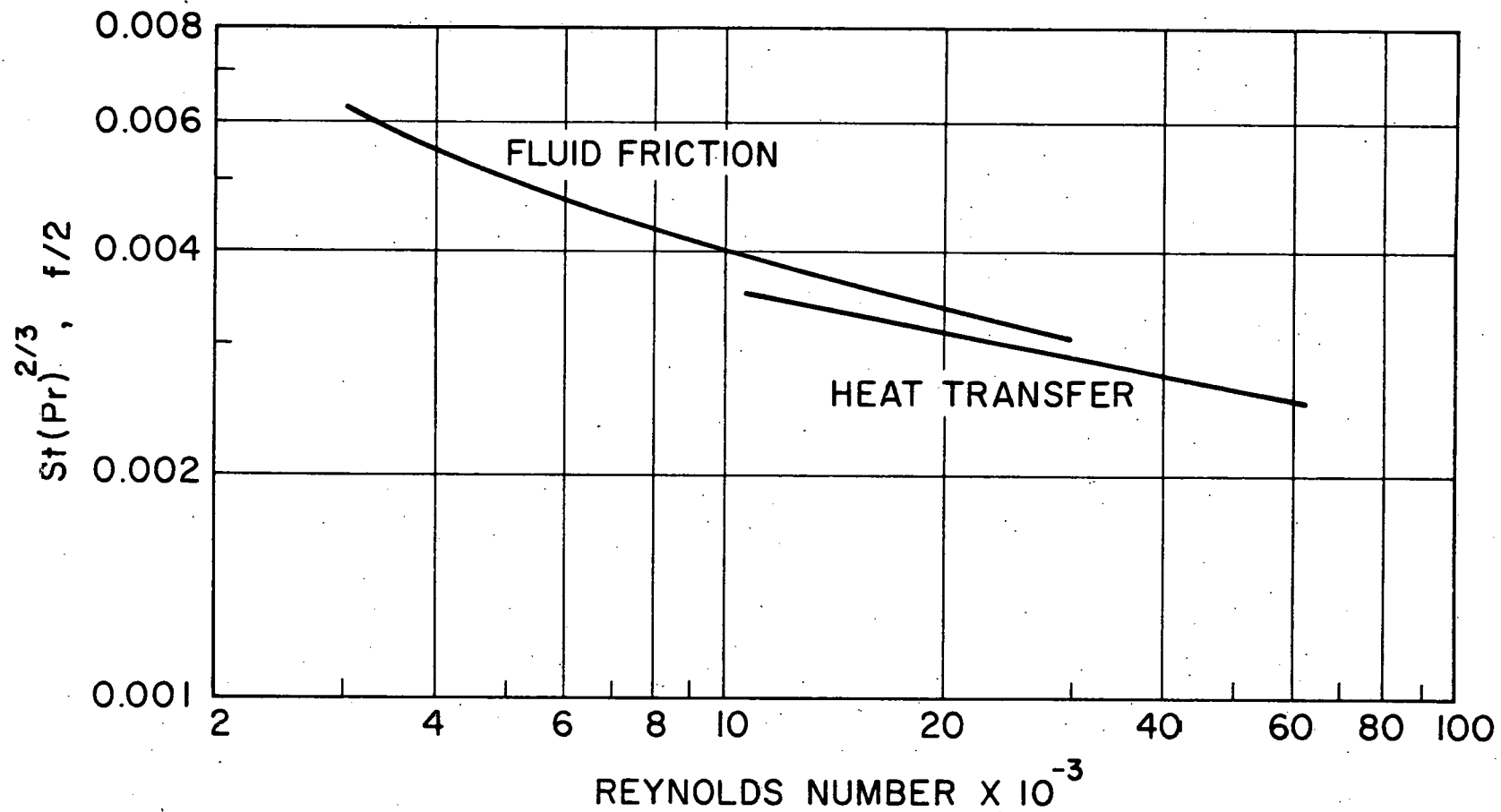


Fig. 6--Comparison of fluid-friction and average heat-transfer data

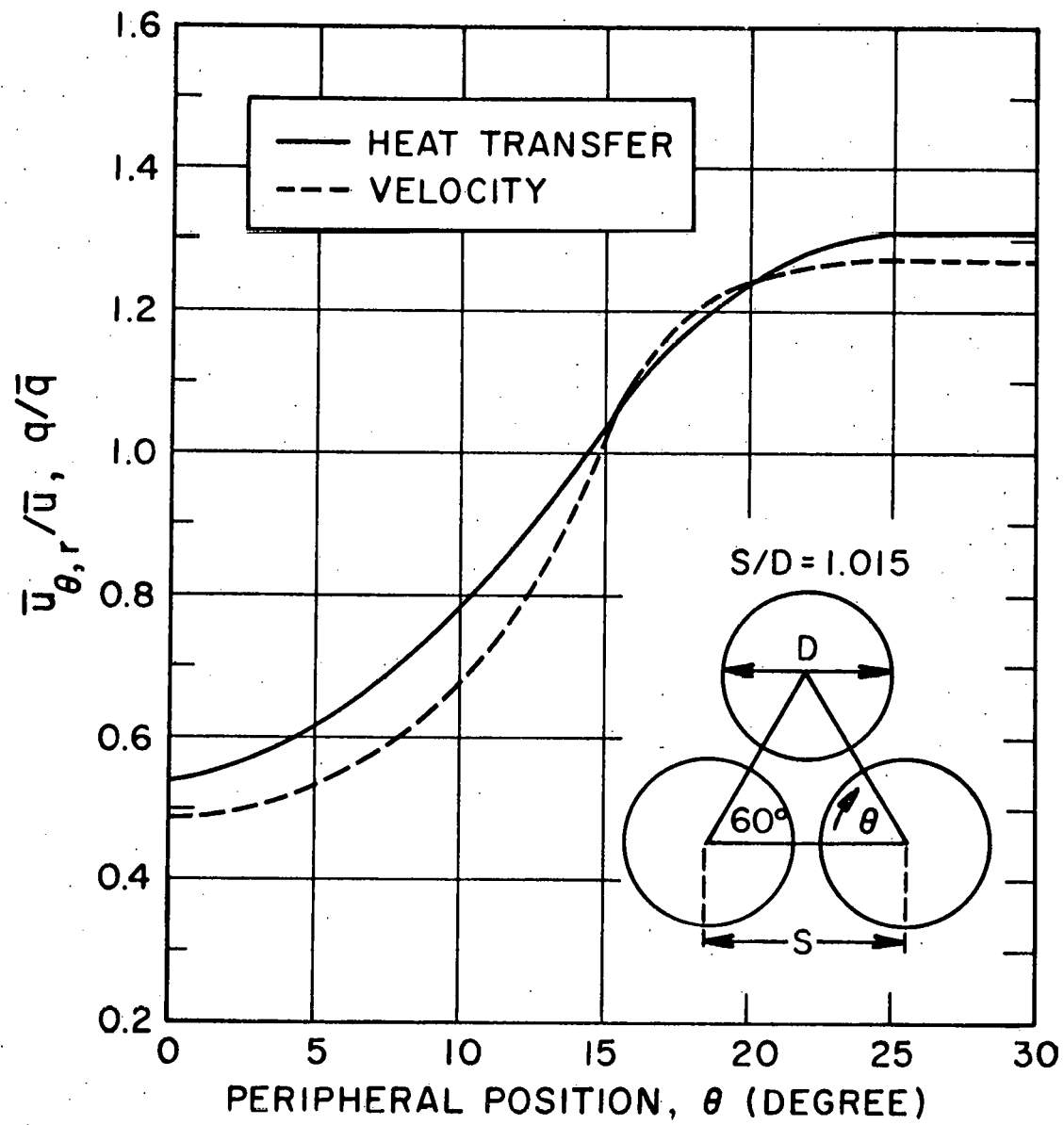


Fig. 7--Comparison of local heat-transfer film coefficients and local mean velocities at a Reynolds number of 20,000

1. Conventional correlations may be used to predict the average heat-transfer coefficients and pressure losses.
2. The local heat-transfer coefficient varies by a factor of approximately three for a Reynolds number of 20,000, the factor becoming progressively less as the air flow rate is increased.

ACKNOWLEDGMENTS

The authors wish to express their appreciation to Dr. P. Fortescue and Mr. C. Rickard for their encouragement and advice during the course of the investigation.

NOTATION

Letters

A = Heat-transfer area, ft^2

c_p = Specific heat, $\text{Btu}/(\text{lb})(^{\circ}\text{F})$

D = Rod diameter, ft

D_e = Equivalent diameter ($4 A/\text{wetted perimeter}$)

f = Fanning friction factor, defined by $f = \frac{\Delta p}{\rho(\bar{u}_B)^2} \frac{D_e g}{2L}$

g = Gravitational constant, ft/hr^2

\bar{h} = Mean heat-transfer film coefficient, $\text{Btu}/(\text{hr})(\text{ft}^2)(^{\circ}\text{F})$

k = Thermal conductivity, $\text{Btu}/(\text{hr})(\text{ft}^2)(^{\circ}\text{F})/\text{ft}$

L = Length, ft

m = Mass flow rate, lb/hr

n = Dimensionless distance from rod surface (perpendicular distance from rod \div perpendicular distance from rod to line of symmetry between rods)

Δp = Differential pressure, lb/ft^2

q = Local rate of heat transfer, Btu/hr

\bar{q} = Mean heat-transfer rate, Btu/hr
 s = Rod pitch spacing, ft
 $t_{m, in}$ = Mixed mean inlet fluid temperature, $^{\circ}$ F
 $t_{x, X}$ = Rod local surface temperature, $^{\circ}$ F
 u = Local velocity, ft/sec
 $\bar{u}_{r, \theta}$ = Local mean velocity, ft/sec
 \bar{u}_B = Bulk or average velocity, ft/sec
 x = Distance from beginning of heated section, ft
 X = Total length of heated section, ft
 θ = Angular position, degrees
 μ = Fluid dynamic viscosity, $lb_m/(hr)(ft)$
 ν = Fluid kinematic viscosity, ft^2/hr
 ρ = Fluid density, lb_m/ft^3

Dimensionless Numbers

Nu = Nusselt number, $\bar{h}D_e/k$
 Pr = Prandtl number, $\mu c_p/k$
 Re = Reynolds number, $D_e \bar{u}/\nu$, $D_e \bar{u}_B/\nu$
 St = Stanton number, $Nu/Re Pr = \bar{h}/c_p \bar{u}_B \rho$

BIBLIOGRAPHY

1. "Analysis of Axial Turbulent Flow and Heat Transfer Through Banks of Rods or Tubes," by Robert G. Deissler and Maynard F. Taylor, Reactor Heat Transfer Conference of 1956: Collected Papers and Reports, John E. Viscardi (comp.), TID-7529 (Pt. 1), Book 2, November 1957, p. 416 ff.
2. "Longitudinal Laminar Flow Between Cylinders Arranged in Regular Array," by E. M. Sparrow and A. L. Loeffler, Jr., American Institute of Chemical Engineers Journal, Vol. 5, No. 3, 1959, p. 325.

3. "Heat Transfer from Parallel Rods in Axial Flow," by David A. Dingee, Wayne B. Bell, Joel W. Chastain, and Sherwood L. Fawcett, Battelle Memorial Institute, BMI-1026, August 5, 1955.
4. "Heat Transfer from Parallel Rods in Axial Flow," by D. A. Dingee and J. W. Chastain, Reactor Heat Transfer Conference of 1956: Collected Papers and Reports, John E. Viscardi (comp.), TID-7529 (Pt. 1), Book 2, November 1957, p. 462 ff.
5. "Heat Transfer to Water Flowing Parallel to a Rod Bundle," by Philip Miller, James J. Byrnes, and David M. Benforado, Paper presented at the Nuclear Engineering and Science Congress, held in December 1955, Preprint by the American Institute of Chemical Engineers, New York.
6. "Pressure Drop Through Parallel Rod Subassemblies Having a 1.12 Equilateral Triangular Pitch," by B. W. Le Tourneau, R. E. Grimble, and J. E. Zerbe, Westinghouse Electric Corp., Atomic Power Division, Report WAPD-TH-118, August 29, 1955.
7. "Measurement of Heat-Transfer and Friction Coefficients for Flow of Air in Noncircular Duct at High Surface Temperatures," by Warren H. Lowdermilk, Walter F. Weiland, Jr., and John N. B. Livingood, National Advisory Committee for Aeronautics (N. A. C. A.), Research Memorandum E53J07, January 25, 1954.
8. "Heat Transmission," by William H. McAdams, 3rd Edition, McGraw-Hill Book Company, Inc., New York, N. Y., 1954, p. 156.
9. "Measurements of Average Heat-Transfer and Friction Coefficients for Subsonic Flow of Air in Smooth Tubes at High Surface and Fluid Temperatures," by Leroy V. Humble, Warren H. Lowdermilk, and Leland G. Desmon, N. A. C. A., Report 1020, 1951.
10. "Correlation of Forced-Convection Heat-Transfer for Air Flowing in Smooth Platinum Tubes with Long Approach Entrance at High Surface and Inlet-Air Temperatures," by L. G. Desmon and E. W. Sams, N. A. C. A., Research Memorandum E50H23, 1950.

11. "Remarks on the Analogy Between Heat Transfer and Momentum Transfer," by L. M. K. Boelter, R. C. Martinelli, and Finn Jonassen, Trans. A.S.M.E., Volume 63, No. 5, 1941, pp. 447-455.

ADDENDUM

DESCRIPTION OF TYPICAL HEAT-TRANSFER ROD AND SURFACE HEATER

Drawings of a typical heat-transfer rod and a surface heater are shown in Figs. 1 and 2. A photograph of the test lattice during assembly is shown in Fig. 3. Engineering drawings of the heat transfer and hydrodynamic systems may be obtained by contacting the authors.

METHOD OF CALIBRATION OF THE SMALL SURFACE HEATER

Measurements of the rate of heat transfer from the inner wall of an annulus to air were made in order to determine the validity and resolution of the technique used in measuring the local and average heat-transfer rates within the rod-bundle test lattice. The central rod of the tube bundle was centered within a tube of 7-5/8-in. inside diameter. The annulus formed, thus, replaced the tube bundle. There were no other changes in the flow system. The heat transfer measurements were made under the following conditions:

Reynolds number 12,000 to 60,000

Inner-wall heat flux 370 to 1,150 Btu/(hr)(ft²)

Rod surface temperature . . . 93° to 130° F

The data for heat transfer in annuli can be correlated if the usual variables plus the ratios of the inner to outer wall diameters are included. Davis* has used a dimensionless grouping to relate several different sizes of annuli and types of fluids; the data obtained in the annulus of this experiment were compared with the Davis correlation (see Fig. 4).

It was found necessary to guard-heat the small surface heater in order to equalize the heat flux from the heater surface to that from the adjacent rod

* "Heat Transfer and Pressure Drop in Annuli," E. S. Davis, Transactions of the A. S. M. E., Vol. 65, No. 7, 1943, pp. 755-759.

surface. This guard-heating prevented an apparent heat loss of about 10%. The amount of guard-heating necessary for flow conditions of interest was determined, and this information was used in the heat-transfer measurements within the tricuspid channels of the test lattice.

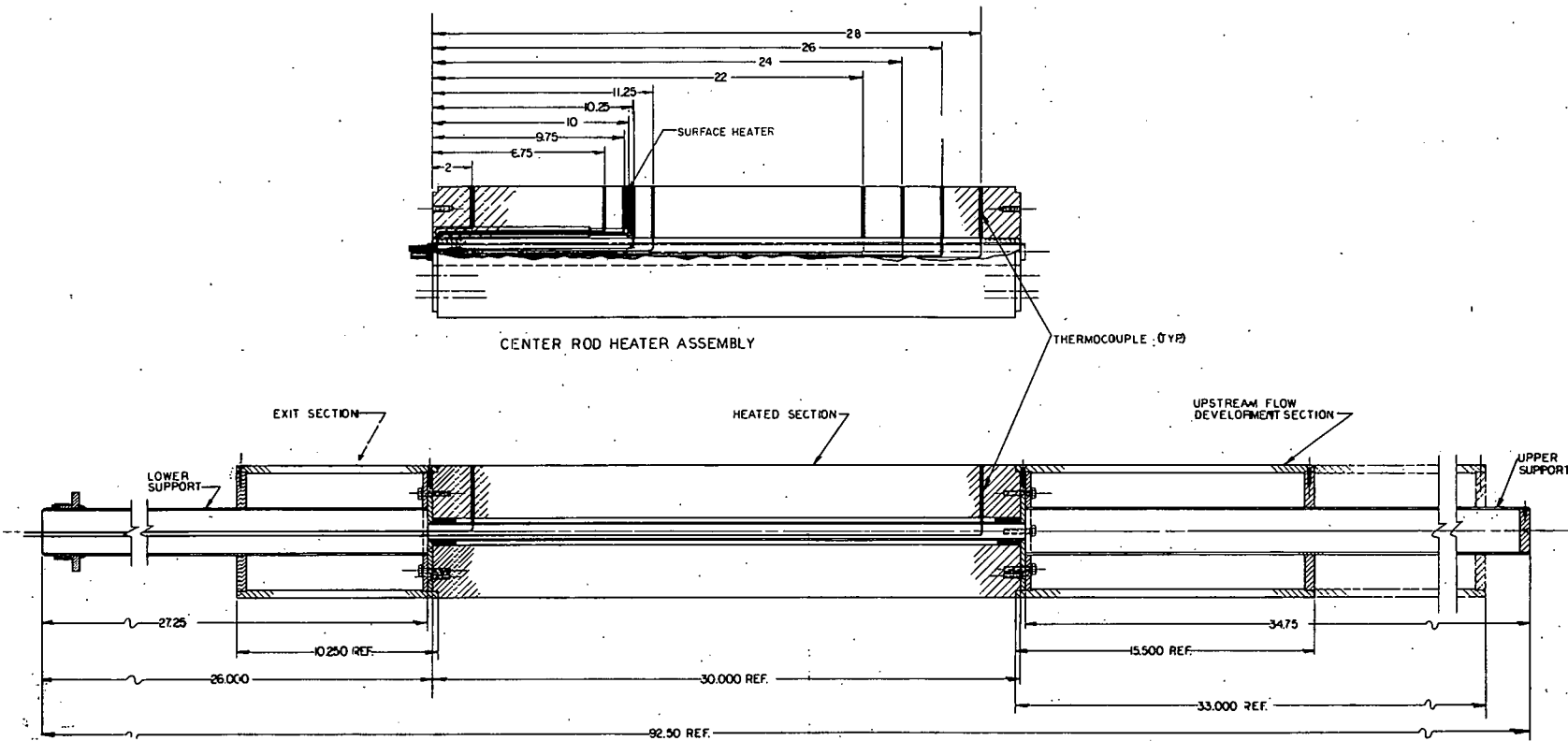
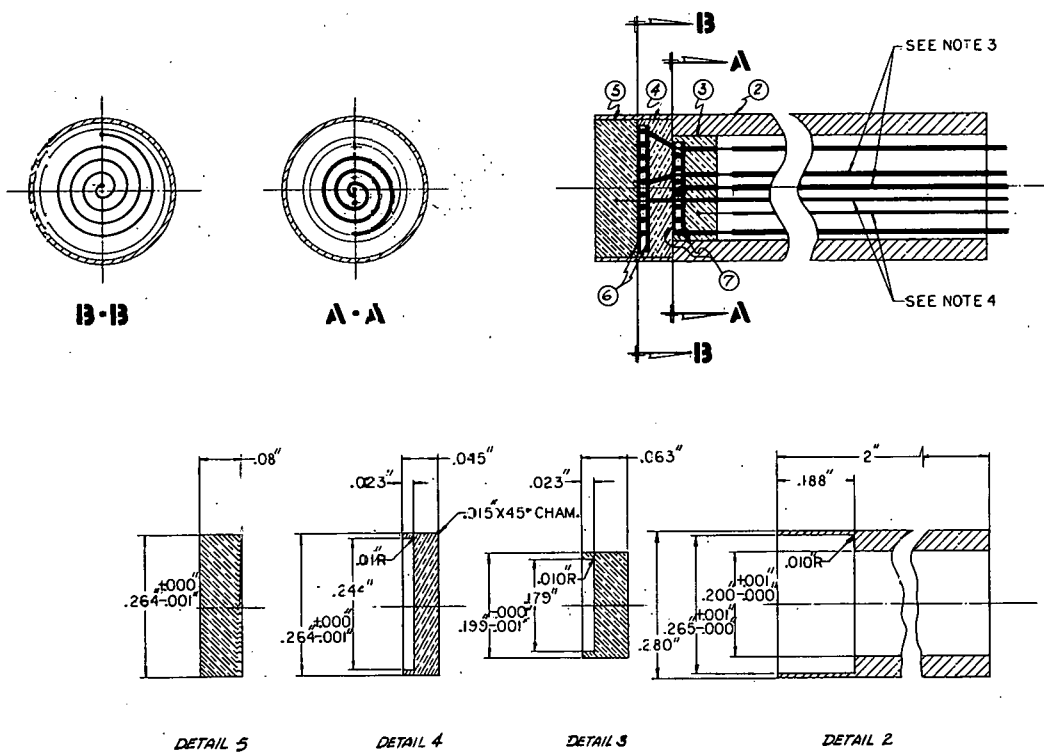


Fig. 1--Drawing of a heat-transfer test rod



NOTES

1. REMOVE ALL BURRS & SHARP EDGES
 2. ITEMS 3 & 5 TO BE GLUED IN PLACE
 3. HEATING COILS TO BE 1 OHM. OR APPROX. 1' (IN LENGTH) OF 32 GA. NICHROME WIRE COILED & INSTALLED AS SHOWN. HOLES FOR ENTRANCE OF WIRE TO BE $\frac{1}{16}$ DIA. & DRILLED AT ASSEMBLY.
 4. THERMOCOUPLES TO BE MADE FROM 36 GA. COPPER-CONSTANTAN WIRE & INSTALLED APPROX. AS SHOWN. WIRE INSULATION DIA. TO DETERMINE DIA. OF HOLES (TO BE DRILLED AT ASSEMBLY) FOR ENTRANCE
 5. THERMOCOUPLE AND HEATING COIL LEADS TO BE APPROX. 15 FT. IN LENGTH TO PERMIT ASSEMBLY IN ELEMENT
 DWG. NO. 32-SK-1295

ITEM	PART NO.	DESCRIPTION	MATL
1	244 DIA X .010	ALUMINA	
2	244 DIA X .015	AL. AL.	
3	244 DIA X .0215	AL. AL.	
4	244 DIA X .0275	AL. AL.	
5	244 DIA X .0325	AL. AL.	
6	244 DIA X .0375	ALUMINA	
7	244 DIA X .0425	ALUMINA	
8	244 DIA X .0475	ALUMINA	
9	244 DIA X .0525	ALUMINA	
10	244 DIA X .0575	ALUMINA	
11	244 DIA X .0625	ALUMINA	
12	244 DIA X .0675	ALUMINA	
13	244 DIA X .0725	ALUMINA	
14	244 DIA X .0775	ALUMINA	
15	244 DIA X .0825	ALUMINA	
16	244 DIA X .0875	ALUMINA	
17	244 DIA X .0925	ALUMINA	
18	244 DIA X .0975	ALUMINA	
19	244 DIA X .1025	ALUMINA	
20	244 DIA X .1075	ALUMINA	
21	244 DIA X .1125	ALUMINA	
22	244 DIA X .1175	ALUMINA	
23	244 DIA X .1225	ALUMINA	
24	244 DIA X .1275	ALUMINA	
25	244 DIA X .1325	ALUMINA	
26	244 DIA X .1375	ALUMINA	
27	244 DIA X .1425	ALUMINA	
28	244 DIA X .1475	ALUMINA	
29	244 DIA X .1525	ALUMINA	
30	244 DIA X .1575	ALUMINA	
31	244 DIA X .1625	ALUMINA	
32	244 DIA X .1675	ALUMINA	
33	244 DIA X .1725	ALUMINA	
34	244 DIA X .1775	ALUMINA	
35	244 DIA X .1825	ALUMINA	
36	244 DIA X .1875	ALUMINA	
37	244 DIA X .1925	ALUMINA	
38	244 DIA X .1975	ALUMINA	
39	244 DIA X .2025	ALUMINA	
40	244 DIA X .2075	ALUMINA	
41	244 DIA X .2125	ALUMINA	
42	244 DIA X .2175	ALUMINA	
43	244 DIA X .2225	ALUMINA	
44	244 DIA X .2275	ALUMINA	
45	244 DIA X .2325	ALUMINA	
46	244 DIA X .2375	ALUMINA	
47	244 DIA X .2425	ALUMINA	
48	244 DIA X .2475	ALUMINA	
49	244 DIA X .2525	ALUMINA	
50	244 DIA X .2575	ALUMINA	
51	244 DIA X .2625	ALUMINA	
52	244 DIA X .2675	ALUMINA	
53	244 DIA X .2725	ALUMINA	
54	244 DIA X .2775	ALUMINA	
55	244 DIA X .2825	ALUMINA	
56	244 DIA X .2875	ALUMINA	
57	244 DIA X .2925	ALUMINA	
58	244 DIA X .2975	ALUMINA	
59	244 DIA X .3025	ALUMINA	
60	244 DIA X .3075	ALUMINA	
61	244 DIA X .3125	ALUMINA	
62	244 DIA X .3175	ALUMINA	
63	244 DIA X .3225	ALUMINA	
64	244 DIA X .3275	ALUMINA	
65	244 DIA X .3325	ALUMINA	
66	244 DIA X .3375	ALUMINA	
67	244 DIA X .3425	ALUMINA	
68	244 DIA X .3475	ALUMINA	
69	244 DIA X .3525	ALUMINA	
70	244 DIA X .3575	ALUMINA	
71	244 DIA X .3625	ALUMINA	
72	244 DIA X .3675	ALUMINA	
73	244 DIA X .3725	ALUMINA	
74	244 DIA X .3775	ALUMINA	
75	244 DIA X .3825	ALUMINA	
76	244 DIA X .3875	ALUMINA	
77	244 DIA X .3925	ALUMINA	
78	244 DIA X .3975	ALUMINA	
79	244 DIA X .4025	ALUMINA	
80	244 DIA X .4075	ALUMINA	
81	244 DIA X .4125	ALUMINA	
82	244 DIA X .4175	ALUMINA	
83	244 DIA X .4225	ALUMINA	
84	244 DIA X .4275	ALUMINA	
85	244 DIA X .4325	ALUMINA	
86	244 DIA X .4375	ALUMINA	
87	244 DIA X .4425	ALUMINA	
88	244 DIA X .4475	ALUMINA	
89	244 DIA X .4525	ALUMINA	
90	244 DIA X .4575	ALUMINA	
91	244 DIA X .4625	ALUMINA	
92	244 DIA X .4675	ALUMINA	
93	244 DIA X .4725	ALUMINA	
94	244 DIA X .4775	ALUMINA	
95	244 DIA X .4825	ALUMINA	
96	244 DIA X .4875	ALUMINA	
97	244 DIA X .4925	ALUMINA	
98	244 DIA X .4975	ALUMINA	
99	244 DIA X .5025	ALUMINA	
100	244 DIA X .5075	ALUMINA	
101	244 DIA X .5125	ALUMINA	
102	244 DIA X .5175	ALUMINA	
103	244 DIA X .5225	ALUMINA	
104	244 DIA X .5275	ALUMINA	
105	244 DIA X .5325	ALUMINA	
106	244 DIA X .5375	ALUMINA	
107	244 DIA X .5425	ALUMINA	
108	244 DIA X .5475	ALUMINA	
109	244 DIA X .5525	ALUMINA	
110	244 DIA X .5575	ALUMINA	
111	244 DIA X .5625	ALUMINA	
112	244 DIA X .5675	ALUMINA	
113	244 DIA X .5725	ALUMINA	
114	244 DIA X .5775	ALUMINA	
115	244 DIA X .5825	ALUMINA	
116	244 DIA X .5875	ALUMINA	
117	244 DIA X .5925	ALUMINA	
118	244 DIA X .5975	ALUMINA	
119	244 DIA X .6025	ALUMINA	
120	244 DIA X .6075	ALUMINA	
121	244 DIA X .6125	ALUMINA	
122	244 DIA X .6175	ALUMINA	
123	244 DIA X .6225	ALUMINA	
124	244 DIA X .6275	ALUMINA	
125	244 DIA X .6325	ALUMINA	
126	244 DIA X .6375	ALUMINA	
127	244 DIA X .6425	ALUMINA	
128	244 DIA X .6475	ALUMINA	
129	244 DIA X .6525	ALUMINA	
130	244 DIA X .6575	ALUMINA	
131	244 DIA X .6625	ALUMINA	
132	244 DIA X .6675	ALUMINA	
133	244 DIA X .6725	ALUMINA	
134	244 DIA X .6775	ALUMINA	
135	244 DIA X .6825	ALUMINA	
136	244 DIA X .6875	ALUMINA	
137	244 DIA X .6925	ALUMINA	
138	244 DIA X .6975	ALUMINA	
139	244 DIA X .7025	ALUMINA	
140	244 DIA X .7075	ALUMINA	
141	244 DIA X .7125	ALUMINA	
142	244 DIA X .7175	ALUMINA	
143	244 DIA X .7225	ALUMINA	
144	244 DIA X .7275	ALUMINA	
145	244 DIA X .7325	ALUMINA	
146	244 DIA X .7375	ALUMINA	
147	244 DIA X .7425	ALUMINA	
148	244 DIA X .7475	ALUMINA	
149	244 DIA X .7525	ALUMINA	
150	244 DIA X .7575	ALUMINA	
151	244 DIA X .7625	ALUMINA	
152	244 DIA X .7675	ALUMINA	
153	244 DIA X .7725	ALUMINA	
154	244 DIA X .7775	ALUMINA	
155	244 DIA X .7825	ALUMINA	
156	244 DIA X .7875	ALUMINA	
157	244 DIA X .7925	ALUMINA	
158	244 DIA X .7975	ALUMINA	
159	244 DIA X .8025	ALUMINA	
160	244 DIA X .8075	ALUMINA	
161	244 DIA X .8125	ALUMINA	
162	244 DIA X .8175	ALUMINA	
163	244 DIA X .8225	ALUMINA	
164	244 DIA X .8275	ALUMINA	
165	244 DIA X .8325	ALUMINA	
166	244 DIA X .8375	ALUMINA	
167	244 DIA X .8425	ALUMINA	
168	244 DIA X .8475	ALUMINA	
169	244 DIA X .8525	ALUMINA	
170	244 DIA X .8575	ALUMINA	
171	244 DIA X .8625	ALUMINA	
172	244 DIA X .8675	ALUMINA	
173	244 DIA X .8725	ALUMINA	
174	244 DIA X .8775	ALUMINA	
175	244 DIA X .8825	ALUMINA	
176	244 DIA X .8875	ALUMINA	
177	244 DIA X .8925	ALUMINA	
178	244 DIA X .8975	ALUMINA	
179	244 DIA X .9025	ALUMINA	
180	244 DIA X .9075	ALUMINA	
181	244 DIA X .9125	ALUMINA	
182	244 DIA X .9175	ALUMINA	
183	244 DIA X .9225	ALUMINA	
184	244 DIA X .9275	ALUMINA	
185	244 DIA X .9325	ALUMINA	
186	244 DIA X .9375	ALUMINA	
187	244 DIA X .9425	ALUMINA	
188	244 DIA X .9475	ALUMINA	
189	244 DIA X .9525	ALUMINA	
190	244 DIA X .9575	ALUMINA	
191	244 DIA X .9625	ALUMINA	
192	244 DIA X .9675	ALUMINA	
193	244 DIA X .9725	ALUMINA	
194	244 DIA X .9775	ALUMINA	
195	244 DIA X .9825	ALUMINA	
196	244 DIA X .9875	ALUMINA	
197	244 DIA X .9925	ALUMINA	
198	244 DIA X .9975	ALUMINA	
199	244 DIA X .0025	ALUMINA	
200	244 DIA X .0075	ALUMINA	
201	244 DIA X .0125	ALUMINA	
202	244 DIA X .0175	ALUMINA	
203	244 DIA X .0225	ALUMINA	
204	244 DIA X .0275	ALUMINA	
205	244 DIA X .0325	ALUMINA	
206	244 DIA X .0375	ALUMINA	
207	244 DIA X .0425	ALUMINA	
208	244 DIA X .0475	ALUMINA	
209	244 DIA X .0525	ALUMINA	
210	244 DIA X .0575	ALUMINA	
211	244 DIA X .0625	ALUMINA	
212	244 DIA X .0675	ALUMINA	
213	244 DIA X .0725	ALUMINA	
214	244 DIA X .0775	ALUMINA	
215	244 DIA X .0825	ALUMINA	
216	244 DIA X .0875	ALUMINA	
217	244 DIA X .0925	ALUMINA	
218	244 DIA X .0975	ALUMINA	
219	244 DIA X .1025	ALUMINA	
220	244 DIA X .1075	ALUMINA	
221	244 DIA X .1125	ALUMINA	
222	244 DIA X .1175	ALUMINA	
223	244 DIA X .1225	ALUMINA	
224	244 DIA X .1275	ALUMINA	
225	244 DIA X .1325	ALUMINA	
226	244 DIA X .1375	ALUMINA	
227	244 DIA X .1425	ALUMINA	
228	244 DIA X .1475	ALUMINA	
229	244 DIA X .1525	ALUMINA	
230	244 DIA X .1575	ALUMINA	
231	244 DIA X .1625	ALUMINA	
232	244 DIA X .1675	ALUMINA	
233	244 DIA X .1725	ALUMINA	
234	244 DIA X .1775	ALUMINA	
235	244 DIA X .1825	ALUMINA	
236	244 DIA X .1875	ALUMINA	
237	244 DIA X .1925	ALUMINA	
238	244 DIA X .1975	ALUMINA	
239	244 DIA X .2025	ALUMINA	
240	244 DIA X .2075	ALUMINA	
241	244 DIA X .2125	ALUMINA	
242	244 DIA X .2175	ALUMINA	
243	244 DIA X .2225	ALUMINA	
244	244 DIA X .2275	ALUMINA	
245	244 DIA X .2325	ALUMINA	
246	244 DIA X .2375	ALUMINA	
247	244 DIA X .2425	ALUMINA	
248	244 DIA X .2475	ALUMINA	
249	244 DIA X .2525	ALUMINA	
250	244 DIA X .2575	ALUMINA	
251	244 DIA X .2625	ALUMINA	
252	244 DIA X .2675	ALUMINA	
253	244 DIA X .2725	ALUMINA	
254	244 DIA X .2775	ALUMINA	
255	244 DIA X .2825	ALUMINA	
256	244 DIA X .2875	ALUMINA	
257	244 DIA X .2925	ALUMINA	
258	244 DIA X .2975	ALUMINA	
259	244 DIA X .3025	ALUMINA	
260	244 DIA X .3075	ALUMINA	
261	244 DIA X .3125	ALUMINA	
262	244 DIA X .3175	ALUMINA	
263	244 DIA X .3225	ALUMINA	
264	244 DIA X .3275	ALUMINA	
265	244 DIA X .3325	ALUMINA	
266	244 DIA X .3375	ALUMINA	
267			

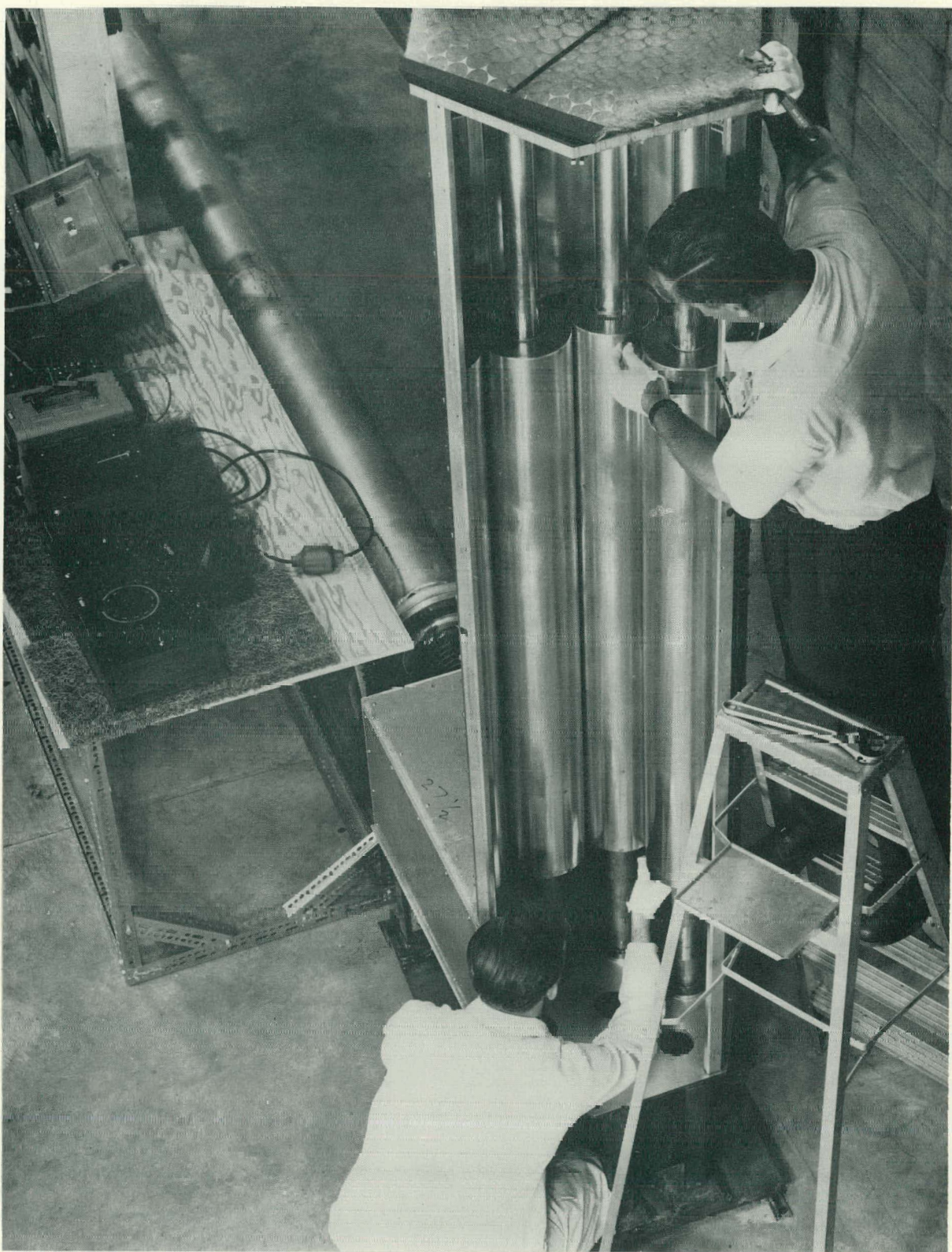
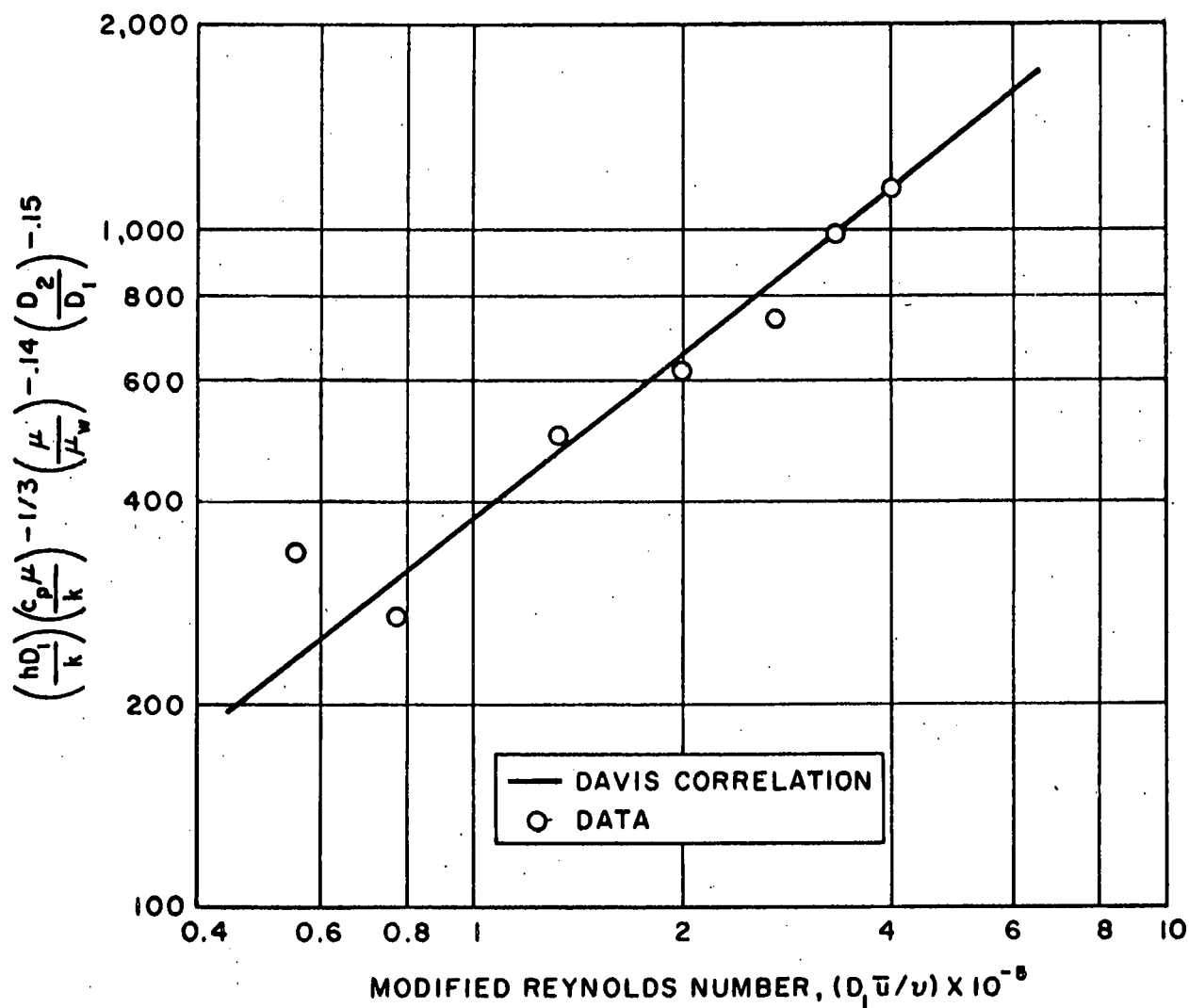


Fig. 3--Heat transfer test lattice



Here, c_p Specific heat, Btu/(lb) ($^{\circ}$ F)

D_1 Inner diameter of annulus, ft

D_2 Outer diameter of annulus, ft

h Mean heat transfer film coefficient, Btu/(hr) (ft^2) ($^{\circ}$ F)

k Thermal conductivity, Btu/(hr) (ft^2) ($^{\circ}$ F)/ft

\bar{u} Average velocity, ft/sec

μ Air dynamic viscosity, lb/(hr) (ft)

μ_w Dynamic viscosity of air at wall, lb/(hr) (ft)

v Air kinematic viscosity, ft^2 /hr

Fig. 4--Comparison of annular heat-transfer data to Davis correlation for turbulent flow